IEEE Access
Multidisciplinary ⋮ Rapid Review ⋮ Open Access Journal

Received November 23, 2020, accepted November 30, 2020, date of publication December 4, 2020, date of current version December 21, 2020.

Digital Object Identifier 10.1109/ACCESS.2020.3042529

Two Dimensional Forward-Looking Missile-Borne Radar Imaging Based on Vortex Electromagnetic Waves

TAOLI YANG, (Member, IEEE), WEI HUANG, AND XINGYU LU
School of Resources and Environment, University of Electronic Science and Technology of China, Chengdu 611731, China

Corresponding author: Taoli Yang (yangtl@uestc.edu.cn)

This work was supported in part by the National Natural Science Foundation of China under Grant 61601090, Grant 41471361, Grant 41371439, and Grant 61601470, and in part by the Shanghai Aerospace Science and Technology Innovation Fund under Grant SAST2016037.

ABSTRACT In this article, a novel two-dimensional (2D) imaging scheme for forward-looking missile-borne radar systems is proposed, where the vortex electromagnetic (EM) waves with different orbital angular momentum (OAM) modes are transmitted. First, the vortex EM waves's radar imaging model is established. Then, two processing algorithms, i.e. the FFT and the sparse recovery algorithms, are proposed. Finally, the simulation results confirm the proposed algorithms. Compared with the traditional missile-borne radar, the OAM-based system can not only achieve the slant range resolution, but also the azimuth resolution. Besides, be different from the traditional 2D synthetic aperture radar (SAR), the azimuth resolution of the novel system is independent from the Doppler bandwidth and can be obtained even at the forward-looking mode.

INDEX TERMS Forward-looking, missile-borne radar, orbital angular momentum (OAM), two-dimensional imaging.

I. INTRODUCTION

Automatic target examination, recognition and tracking is the main development direction in equipments of modern military weapons, and missile is one of the most important weapons. A missile can be guided to a target by guidance signals developed from tracking data. For a missile homing guidance system, the tracking data and guidance signals can be provided by a radar system. In one type of missile homing guidance system, both the radar transmitter and receiver are located in the missile, which can be called as missile-borne monostatic radar. In another type of homing system, the radar transmitter is located remotely from the missile, while the receiver is located in the missile, which can be called as missile-borne bistatic radar. Prior art missile-borne radar systems have been designed to obtain high discrimination in angle and in range by monopulse of "beam splitting" methods. Such methods are valid only if there is only one target inside the pulse volume. When there are more than one target in the volume, these systems will fail.

The associate editor coordinating the review of this manuscript and approving it for publication was Ravibabu Mulaveesala.

With the increasing requirement of high precision guidance capability, the missile-borne radar is urged to achieve the two-dimensional (2D) images of the interested targets. Because of the cloud-penetration and day and night working capabilities, synthetic aperture radar (SAR) has been attracting more and more attentions [1]. The traditional SAR systems achieve high range resolution by transmitting linear frequency modulation (LFM) signal and using the traditional pulse compression method. The azimuth resolution can be obtained by processing the Doppler bandwidth arising from the relative motion between the radar and the targets. Normally, in order to achieve good performance in azimuth, most of traditional SAR systems are designed to work at side-looking or low-squinted modes. Nevertheless, the missile-borne radar can only work at forward-looking or high-squinted modes with the consideration of limited yaw angles. If working at forward-looking mode, SAR has no azimuth resolution. In order to solve such problem, the bistatic forward-looking SAR is proposed [2]–[4]. The transmitter and the receivers are placed at two platforms, and the transmitter works at forward-looking mode, while the receiver works at side-looking mode. Such configuration can be regarded as a high-squinted mode. The most intractable

This work is licensed under a Creative Commons Attribution 4.0 License. For more information, see https://creativecommons.org/licenses/by/4.0/

problem of the high-squinted SAR is the serious coupling between the azimuth and range signal. The larger the squint angle is, the coupling phenomenon is more serious and the achieved azimuth resolution is coarser. There are quite a few literatures proposed to study the high-squinted issues. However, the squint angles are limited to 50 degree or lower in most of the available literatures [3], [5], [6].

Recently, orbital angular momentum (OAM) has attracted more and more attention in different fields, such as wireless communication, nanotechnology, and quantum experiments, because OAM can offer a new degree of freedom besides of the traditional linear momentum and polarization [7]. Usually, a beam carrying OAM is called as vortex electromagnetic (EM) wave since it has a 'doughnut' intensity shape and helical wave front [8]. For radar imaging, the vortex EM wave was utilized firstly in [9]. Subsequently, the phase front distribution of the vortex EM wave and the 2D imaging method are investigated [10], [11]. Considering the relative motion between the radar and targets, the 3D imaging methods based on OAM are studied in [12], [13]. In [14], a scheme for adjusting the directivity of electromagnetic vortex beam is proposed. The vortex EM wave with OAM is used to improve the azimuth resolution of SAR imaging [15], [16], and can also be applied to the MIMO-SAR system, where the different OAM modes can be taken as the orthogonal signals [17]. In [18], the OAM-based InSAR technique is studied.

In this article, a novel OAM-based forward-looking missile-borne radar system is proposed to achieve the 2D image of the interested targets, as well as two processing methods. This arrangement has two advantages. The first one is that it can achieve two dimensional images of the interested targets, while the traditional missile-borne radar is designed to obtain high discrimination only in range. The second one is that the proposed method is independent from the Doppler bandwidth and the dwell time in azimuth, which are key factors for traditional 2D SAR imaging systems. Therefore, the OAM-based system can work at the forward-looking mode, while the SAR systems can only work at side-looking or low-squinted modes. Besides, the traditional SAR imaging problems, such as the range cell migration, are not existed for the OAM-based system. Although there are still many challenging problems to be solved for the OAM-based radar systems, such as the wave generation and long distance transmission, the potential applications of OAM wave are widely studied, and they have shown great potentialities.

This article is organized as follows. The signal model is derived in Section II. In Section III, two processing methods, i.e. FFT method and sparse recovery method, are illustrated. In Section IV, the simulation experiments are carried out to confirm the proposed method. Conclusions are given in Section V.

II. SIGNAL MODEL

In this section, the imaging scenario and the echo model of the OAM-based missile-borne radar system is described.

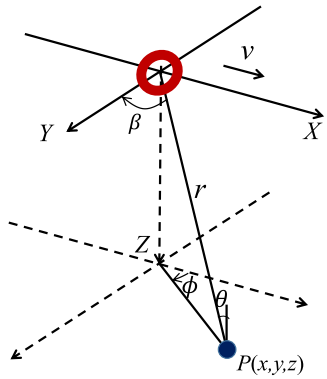

FIGURE 1. Imaging geometry of an OAM-based radar imaging system.

The geometry of the radar system is shown in Fig.1. The missile travels along the X-axis with a speed v. Z-axis points down to the Earth's center, and Y-axis points to the right, completing the orthogonal, right-handed frame. The radar works at forward looking mode. r is the slant range from the sensor to the target. Angles θ, ϕ and β denote the incidence, azimuth and squint angles, respectively. According to the imaging geometry, the relationship between the three angles are

$$\sin(\beta) = \sin(\theta)\cos(\phi). \tag{1}$$

For the target in the beam illuminating center, its squint angle is $\beta = 90°$, and the azimuth angle is $\phi = 0°$. Limited by the working mode and the beamwidth of the radar, the azimuth angle ϕ is usually within about $\pm 20°$. For the visibility, the azimuth angle ϕ is exaggerated in the Fig.1.

The single uniform circular array (UCA) can be used to generate vortex EM waves. However, with the increasement of OAM modes, the direction angle of the maximum gain becomes wider, that is to say, the targets may not be illuminated by the main lobe of the OAM beams [11]. To overcome this problem, the concentric UCA (CUCA) can be deployed. With the proper design, the main lobes of vortex beams with different mode numbers can be collimated to the same elevation direction. In fact, if the elevation angle is not sensitive, or the gain loss of the targets can be ignored, the single UCA is enough. In this article, the concentric uniform circular array (UCA) is utilized to generate vortex EM waves. The detailed antenna design and beam generation can be found in [11], [14].

By using appropriate radiation pattern design methods, the transmitting linear frequency modulation (LFM) signal of each antenna can be written as [12]

$$s_{tr,n}(\tau, l) = \frac{A_l}{N_l} w_r(\tau) \exp\left(j2\pi f_c \tau + j\pi \gamma_r \tau^2\right) \cdot \exp(jl\phi_n). \tag{2}$$

where τ is the range time, l is topology charge or OAM mode number, A_l is the signal amplitude of the beam with topological charge l, N_l is the number of elements for generating

vortex beam with OAM mode l, w_r is the range envelop, f_c is the carrier frequency, γ_r is the linear frequency modulation ratio, and $\phi_n = 2\pi n/N_l$ $(n = 0, 1, \cdots, N_l - 1)$ is the modulation phase of the nth element.

Assuming that there is a target $P(x_T, y_T, z_T)$ located in the detection area, and its corresponding polar coordinates are (r, θ, ϕ). The antenna phase center (APC) of the radar is located at the origin at time $t = 0$. At time t, the received signals of all the antennas after summing over and demodulation can be expressed as [11]

$$\begin{aligned} s_{re}(\tau, l, t) = {} & \sigma(x_T, y_T, z_T) A_l^2 J_l^2(ka_l \sin\theta) \exp(jl\pi) \\ & \cdot w_r\left(\tau - \frac{2r(t)}{c}\right) w_a\left(t - \frac{x_T}{v}\right) \\ & \cdot \exp\left[-j\frac{4\pi r(t)}{\lambda} + j\pi\gamma_r\left(\tau - \frac{2r(t)}{c}\right)^2\right] \\ & \cdot \exp(j2l\phi(t)), \end{aligned} \tag{3}$$

where $\sigma(x_T, y_T, z_T)$ is the complex reflectivity of the scatter, $J_l(ka_l \sin\theta)$ denotes the lth order Bessel function of the first kind, $\lambda = c/f_c$ is the wavelength, $k = 2\pi/\lambda$ is the wave number, c is the propagation velocity, a_l is the radius of the array ring for generating OAM mode l, and w_a is the along-track envelop. $\phi(t)$ is the instantaneous azimuth angle, and can be expressed as

$$\phi(t) = \arccos \frac{(x_T - vt)}{\sqrt{(x_T - vt)^2 + y_T^2}} \tag{4}$$

$r(t)$ is the instantaneous slant range from the radar to the target, and

$$r(t) = \sqrt{(x_T - vt)^2 + y_T^2 + z_T^2} \tag{5}$$

For the traditional SAR imaging system, the azimuth resolution ρ_{SAR} is depended on the Doppler bandwidth B_d, that is

$$\rho_{SAR} = \frac{v}{B_d}. \tag{6}$$

Assume that there is a point-like target P in the illuminating scene as shown in Fig.2, and the radar moves from A to B during the beam dwell time t. The Doppler bandwidth is

$$\begin{aligned} B_d &= \frac{2v}{\lambda}[\sin(\beta_1) - \sin(\beta_2)] \\ &= \frac{2v}{\lambda}[\sin(\beta_1) - \sin(\beta_1 - \Delta\phi)] \end{aligned} \tag{7}$$

where β_1 and β_2 are the squint angles of the radar at position A and B corresponding to the target P, $\Delta\phi = \beta_1 - \beta_2$ is the azimuth angle variation of target P during the illuminating time. Usually, $\Delta\phi$ is small, (7) can be rewritten as

$$B_d \approx \Delta\phi \cos\beta_1 \tag{8}$$

Substituting (8) into (6),

$$\rho_{SAR} = \frac{v}{\Delta\phi \cos\beta_1}. \tag{9}$$

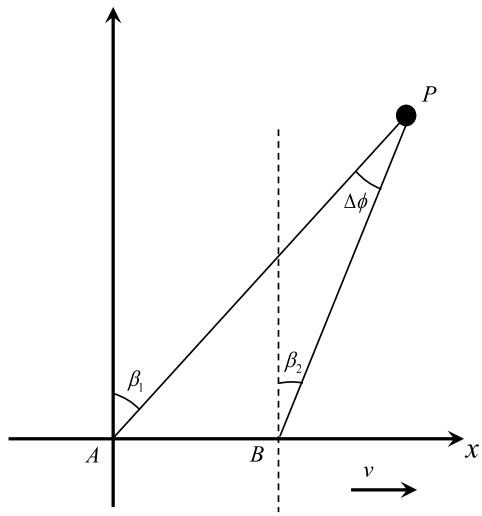

FIGURE 2. The 2D imaging geometry of SAR systems.

From (9), it can be seen that with the increasing of the squint angle, the azimuth resolution is becoming more and more coarse. For large squint angles, although there is azimuth resolution in theory, the coupling phenomenon between range and azimuth signals is serious. When the squint angle approaches to 90°, the radar is blind in azimuth, and all the traditional methods will fail.

III. PROCESSING ALGORITHM

In order to achieve 2D radar images under the forward looking mode, the imaging methods based on OAM waves are proposed in this section, and the flow chart is shown in Fig.3. For a certain azimuth cell, the received echo is compressed in range firstly. Then two different methods can be utilized to compress the echo in OAM domain to obtain the azimuth information. By now, the 2D focused image is obtained. In order to improve the performance, the focused image from other azimuth cells can be integrated. The detailed processing procedures are illustrated in the following.

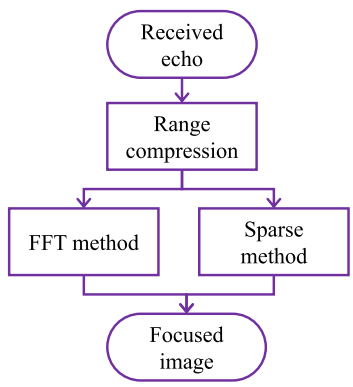

FIGURE 3. The flowchart of the proposed OAM-based method.

A. RANGE COMPRESSION

For the slant range direction, applying the traditional range compression technology, the range profile of the target can

be obtained and the output signal is

$$s_{rc}(\tau, l, t) = \sigma(x_T, y_T, z_T) A_l^2 J_l^2(ka_l \sin\theta) \exp(jl\pi) \cdot p_r\left(\tau - \frac{2r(t)}{c}\right) w_a\left(t - \frac{x_T}{v}\right) \cdot \exp\left(-j\frac{4\pi r(t)}{\lambda}\right) \exp\left(j2l\phi(t)\right), \quad (10)$$

where $p_r(\tau)$ is the range compressed pulse envelope.

For a fixed t and ignoring the symbol t, (10) can be rewritten as

$$s_{rc}(\tau, l) = Bp_r\left(\tau - \frac{2r}{c}\right) \exp\left(j2l\phi\right), \quad (11)$$

where

$$B = \sigma(x_T, y_T, z_T) A_l^2 J_l^2(ka_l \sin\theta) p_r\left(\tau - \frac{2r}{c}\right) \cdot \exp\left(-j\frac{4\pi r}{\lambda}\right) \exp(jl\pi) \quad (12)$$

By compensating an appropriate amplitude term $A_l^2 J_l^2 (ka_l \sin\theta)$ and phase term $\exp(jl\pi)$, B can be regarded as a variable that does not vary with the OAM mode l.

Observing the last term in (11), the variables l and ϕ are dual variables. That is to say, the azimuth angle ϕ of the target can be achieved by using appropriate processing on l. In this article, the FFT method and the sparse recovery method are proposed to obtain the azimuth image.

B. FFT METHOD

Applying Fast Fourier transform (FFT) on l of (11), one gets

$$S_{rc}(\tau, f_l) = Bp_r\left(\tau - \frac{2r}{c}\right) p_a\left(f_l - \frac{\phi}{\pi}\right) \quad (13)$$

So far, the 2D image of the target is obtained. The FFT method is very efficient, however, the resolution is limited. The azimuth angular resolution of the FFT method is

$$\rho_\phi = 0.886\frac{\pi}{\Delta l}, \quad (14)$$

and the corresponding spatial resolution is

$$\rho_a = 0.886 r \sin\theta \frac{\pi}{\Delta l}, \quad (15)$$

where Δl is the range of the OAM modes, and the resolution is evaluated at -3dB level.

Fig.4 shows the azimuth resolution varying with the number of OAM modes, where the system parameters in Table.1 are taken as an example. Generally speaking, the resolution of FFT method is coarse, for example, if the number of OAM modes is 16, the angular resolution is about 9.97°, and the spatial resolution is about 301m. In order to improve the azimuth resolution, more OAM modes should be utilized and the burden of the system is unavoidably heavy. As far as we know, the largest available OAM mode can be reached to ±56 in theory simulations [19], [20], and the available OAM mode is about ±10 in most of the literatures [21], [22]. In the real experiments, the OAM modes from 1 to 7 have been verified [23].

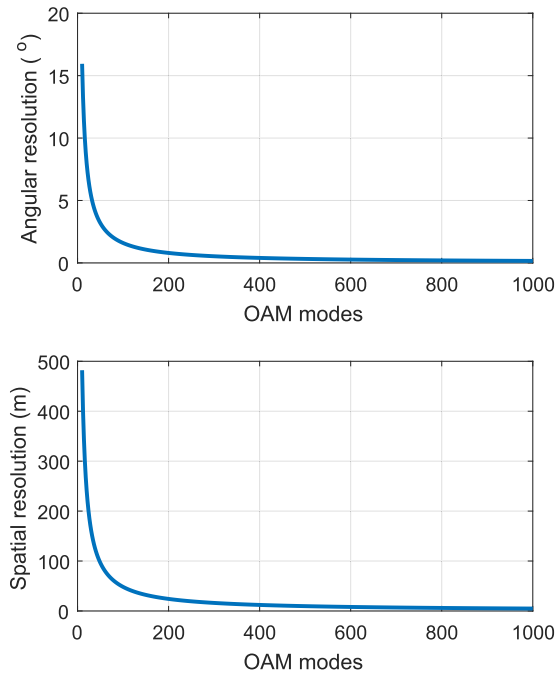

FIGURE 4. The variation of azimuth resolution with the number of OAM modes.

TABLE 1. Simulation Parameters.

PARAMENT	VALUE
Platform height H	1 km
Carrier frequency f_c	35 GHz
Pulse bandwidth B_r	150 MHz
Antenna size in azimuth d_a	0.2 m
Nadir angle of the beam center θ_c	60 °
Squint angle of the scene center β_c	90 °
Slant range of the scene center R_c	2 km
Signal to noise ratio (SNR)	-10 dB

C. SPARSE RECOVERY METHOD

Taking the white noise into account, and assuming that a fixed range cell contains K scattering centers, and the number of OAM modes is N, the received signal of OAM mode l_n ($n = 1, 2, \cdots, N$) can be written as

$$s_{rc}(l_n) = \sum_{k=1}^{K} B_k \exp\left(j2l_n\phi_k\right) + z(l_n), \quad (16)$$

where $z(l_n)$ is the white noise. For different targets, the azimuth angle ϕ_k is different. Using the vector format, (16) can be rewritten as

$$\mathbf{s} = \mathbf{Pb} + \mathbf{z}, \quad (17)$$

where $\mathbf{s}$ is the vector formed by the received signal of different OAM modes,

$$\mathbf{s} = [s_{rc}(l_1), s_{rc}(l_2), \cdots, s_{rc}(l_N)]^T, \quad (18)$$

$$\mathbf{P} = [\mathbf{p}_1, \mathbf{p}_2, \cdots, \mathbf{p}_K] \tag{19}$$
$$\mathbf{p}_k = [\exp(j2l_1\phi_k), \cdots, \exp(j2l_N\phi_k)]^T \tag{20}$$
$$\mathbf{b} = [B_1, \cdots, B_K)]^T \tag{21}$$
$$\mathbf{z} = [z(l_1), z(l_2), \cdots, z(l_N)]^T, \tag{22}$$

The superscript T denotes the transpose operation.

Generally speaking, the number of the interested targets are usually sparse for the missile-borne radar. In this case, the sparse recovery method can be adopted, and the received signal can be converted into the following sparse representation problem [24],

$$\mathbf{s} = \tilde{\mathbf{P}}\tilde{\mathbf{b}} + \mathbf{z} \tag{23}$$

where $\tilde{\mathbf{P}} \in \mathrm{C}^{N\times Q}$ is an overcomplete basis indicating all possible signal,

$$\tilde{\mathbf{P}} = [\tilde{\mathbf{p}}_1, \tilde{\mathbf{p}}_2, \cdots, \tilde{\mathbf{p}}_Q], \tag{24}$$
$$\tilde{\mathbf{p}}_q = [\exp(j2l_1\tilde{\phi}_q), \exp(j2l_2\tilde{\phi}_q), \cdots, \exp(j2l_N\tilde{\phi}_q)]^T \tag{25}$$

Q is the number of all the potential signal vectors. $\tilde{\phi} = \tilde{\phi}_1, \tilde{\phi}_2, \cdots, \tilde{\phi}_Q$ is a sampling grid of all possible target signal directions of interest. $\tilde{\mathbf{b}}$ is the corresponding coefficient sparse vector, whose qth element is nonzero and is equal to the kth element of $\mathbf{b}$ if signal k comes from $\tilde{\phi}_q$ for some k and zero otherwise.

$$\tilde{\mathbf{b}} = [B_1, B_2, \cdots, B_Q)]^T \tag{26}$$

Generally speaking, the number of potential direction Q is much larger than that of the targets to be estimated K.

It should be noted that $\tilde{\mathbf{P}}$ can be constructed according to the assumed target directions. Therefore, the coefficients of the targets can be recovered by solving the following convex problem as

$$\min\left(\|\tilde{\mathbf{b}}\|_1\right), \quad \text{subject to } \|\mathbf{s} - \tilde{\mathbf{P}}\tilde{\mathbf{b}}\|_2 \le \varepsilon \tag{27}$$

where $\|\cdot\|_1$ and $\|\cdot\|_2$ represent ℓ_1-norm and ℓ_2-norm, respectively, and ε is the noise level. The problem in (27) is a convex optimization problem, which can be solved by quite a few of efficient algorithms [25].

It should be noted that since only one azimuth cell is used to obtain the 2D image, there is no need to consider the traditional SAR imaging problems, such as the range cell migration. Besides, the focusing result is not depended on the missile velocity or the height if the location of the target is not considered. In order to eliminate the noise effect and improve the processing performance, the adjacent azimuth cell can also be utilized to repeat the above processing and obtain the several 2D images.

IV. EXPERIMENT

In this section, the simulated data of a missile-borne Ka-band radar is processed to validate the performance of the proposed method. The radar works at the forward-looking mode, i.e., the squint angle of the scene center is 90°. The platform height of the missile is 1km above ground surface. The LFM signal of 150MHz bandwidth is transmitted to ensure a slant range resolution of 1m. The antenna size in azimuth is 0.2m. The slant range of the scene center is 2km, and the nadir angle is 60°. The imaging geometry is shown by Fig.1. The radar position at time $t = 0$ is taken as the origin of the coordinate. Three point-like targets are located in the scene shown in Fig. 5, and their polar coordinates are (2000m, 60°, −0.8185°), (2000m, 60°, 0°) and (2000m, 60°, 0.8185°), respectively. It is obvious that the slant range of the targets to the radar are the same, and their echoes are overlapped together. Therefore, the traditional 1D imaging technique cannot discriminate the three targets. The simulation parameters are summarized in Table 1. The white noise is considered in the simulation, and the signal to noise ratio (SNR) is set to be -10dB before compression. Fig.6 shows the result of range compression. After the coherent processing, the SNR of the image is improved.

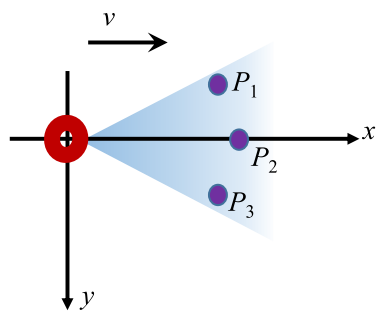

FIGURE 5. The coordinates of the simulated targets.

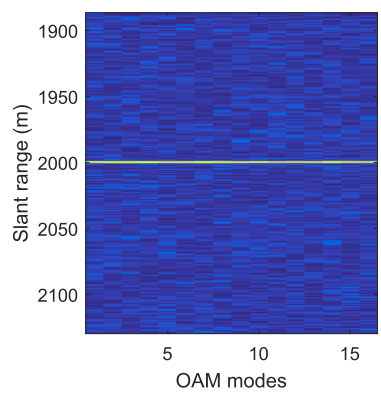

FIGURE 6. Imaging result after range compression.

A. FFT METHOD

According to (14), the number of OAM modes should be larger than 195 in order to distinguish the three targets, if the FFT method is adopted. When the number of OAM modes is smaller than 195, the targets will be overlapped together.

Fig.7 shows the imaging result using the FFT method with 16 OAM modes, where the theoretic azimuth angular resolution is 9.97°, and only one target is observed from the

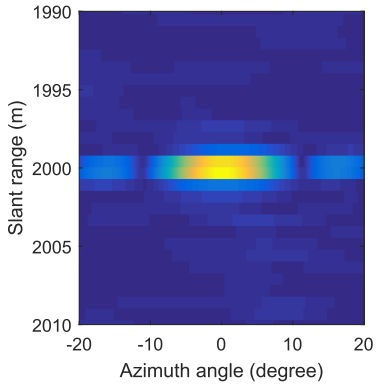

(a) imaging result

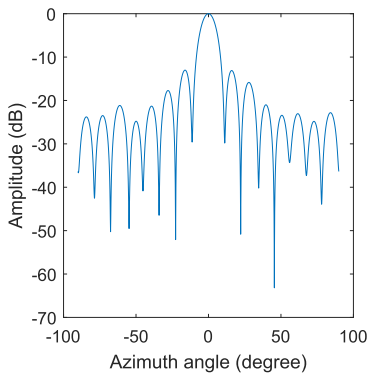

(b) azimuth profile

FIGURE 7. Imaging result using FFT method with N = 16.

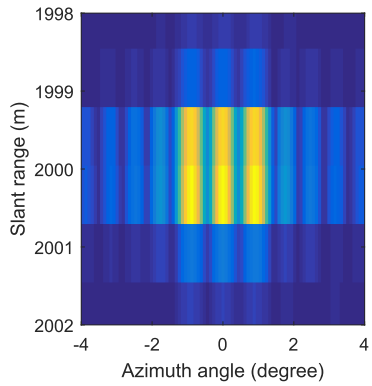

(a) imaging result

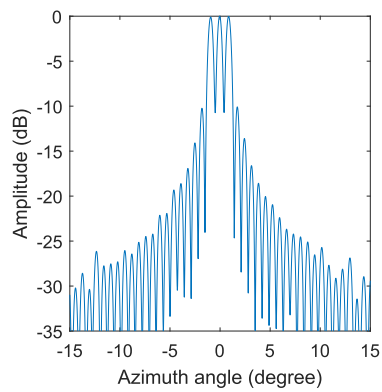

(b) azimuth profile

FIGURE 8. Imaging result using FFT method with N = 256.

imaging result. That is to say, the three targets are overlapped together and hard to be discriminated.

When the number of OAM modes is increased to 256, the theoretic azimuth angular resolution is improved to about 0.623°, and the three targets can be clearly distinguished, as shown by Fig.8.

B. SPARSE RECOVERY METHOD

The FFT method is very efficient, but it has strick requirement for the number of OAM modes. In order to release the system requirement and increase the azimuth resolution, the sparse recovery method can be adopted. In the simulation, only one snapshot at $t = 0$ is adopted. Fig. 9 shows the imaging result using the sparse recovery method, and the number of OAM modes is 16. It can be seen that the three targets are well distinguished.

Be different from the traditional SAR imaging, only one pulse is needed for the OAM system, and the intractable problems such as range cell migration correction (RCMC) are no longer existed. Besides, since the azimuth resolution is not dependent on the Doppler bandwidth, it can also achieve the 2D images at the forward-looking mode.

C. PERFORMANCE ANALYSIS

The processing performance of different methods is evaluated in this section. The reconstructed azimuth angular position, the azimuth angular resolution and the azimuth pulse side-lobe ratio (PSLR) of the targets are displayed in Table.2, Table.3, and Table.4, respectively, where FFT16 and FFT256 represent the processing results using FFT method with 16 OAM modes and 256 OAM modes, respectively, and Sparse16 denotes the sparse method with 16 OAM modes. MAE is the abbreviation of mean absolute error, which is used to evaluate the reconstructed azimuth angular position error, and is defined by the following

TABLE 2. Reconstructed Position of the Targets.

	FFT16	FFT256	Sparse16
Target 1	0.0151°	−0.9375°	−0.8271°
Target 2	0.0151°	−0.0425°	−0.0127°
Target 3	0.0151°	0.8524°	0.7971°
MAE	0.5507°	0.0651°	0.0142°

$$\mathrm{MAE} = \frac{\sum_{k=1}^{K} |\phi_k' - \phi_k|}{K}, \tag{28}$$

where ϕ_k' is the reconstructed azimuth angular position of the kth target.

It can be seen that the sparse recovery method has better performance even with less OAM modes. However, the sparse

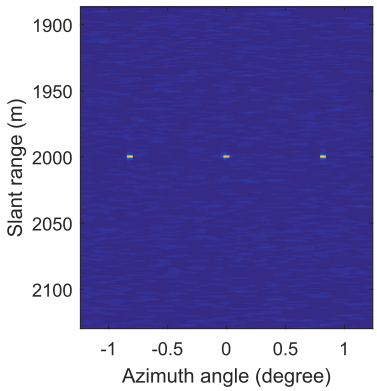

(a) imaging result

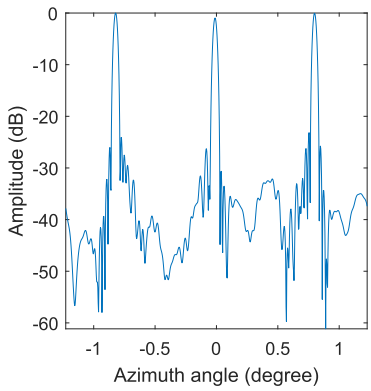

(b) azimuth profile

FIGURE 9. **Imaging result using sparse recovery method with N = 16.**

TABLE 3. **Azimuth Angular Resolution of the Targets.**

	FFT16	FFT256	Sparse16
Target 1	9.9619°	0.4971°	0.0300°
Target 2	-	0.4667°	0.0307°
Target 3	-	0.5019°	0.0299°

TABLE 4. **Azimuth PSLR of the Targets.**

	FFT16	FFT256	Sparse16
Target 1	-12.18dB	-10.49dB	-22.38dB
Target 2	-	-	-28.79dB
Target 3	-	-10.15dB	-22.07dB

recovery method has heavier computation load, and the selection of the noise level ε is also an intractable problem.

V. CONCLUSION

Because of the special working mode, the traditional missile-borne SAR cannot achieve the 2D image in the forward-looking direction, and suffers serious coupling between azimuth and range in the highly squinted direction. In this article, the vortex EM wave with OAM is used for 2D radar imaging. Just like the traditional SAR imaging, the range resolution is obtained by compressing the LFM signal, while the azimuth resolution is obtained according to the dual relationship between the azimuth angle and the OAM modes instead of the Doppler bandwidth. Two methods, FFT method and the sparse recovery method, are proposed to focus the target in azimuth angle direction. Finally, the simulation experiments are carried out to verify the proposed method.

REFERENCES

[1] I. G. Cumming and F. H. Wong, *Digital Processing of Synthetic Aperture Radar Data: Algorithms and Implementation*. Boston, MA, USA: Artech House, 2005.

[2] W. W. Camp, J. T. Mayhan, and R. M. O'Donnell, "Wideband radar for ballistic missile defense and range-Doppler imaging of satellites," *Lincoln Lab. J.*, vol. 12, no. 2, pp. 267–280, 2000.

[3] S. Chen, Y. Yuan, S. Zhang, H. Zhao, and Y. Chen, "A new imaging algorithm for forward-looking missile-borne bistatic SAR," *IEEE J. Sel. Topics Appl. Earth Observ. Remote Sens.*, vol. 9, no. 4, pp. 1543–1552, Apr. 2016.

[4] S. Tang, H. Deng, P. Guo, Y. Li, and L. Zhang, "Generalized PFA for air-missile borne bistatic forward-looking beam-steering SAR with accelerations," *IEEE Access*, vol. 6, pp. 74616–74627, 2018.

[5] S. Tang, L. Zhang, P. Guo, and Y. Zhao, "An omega-K algorithm for highly squinted missile-borne SAR with constant acceleration," *IEEE Geosci. Remote Sens. Lett.*, vol. 11, no. 9, pp. 1569–1573, Sep. 2014.

[6] S. Chen, S. Zhang, H. Zhao, and Y. Chen, "A new chirp scaling algorithm for highly squinted missile-borne SAR based on FrFT," *IEEE J. Sel. Topics Appl. Earth Observ. Remote Sens.*, vol. 8, no. 8, pp. 3977–3987, Aug. 2015.

[7] S. Mohaghegh Mohammadi, L. K. S. Daldorff, J. E. S. Bergman, R. L. Karlsson, B. Thide, K. Forozesh, T. D. Carozzi, and B. Isham, "Orbital angular momentum in radio—A system study," *IEEE Trans. Antennas Propag.*, vol. 58, no. 2, pp. 565–572, Feb. 2010.

[8] L. Allen, M. W. Beijersbergen, R. J. C. Spreeuw, and J. P. Woerdman, "Orbital angular momentum of light and the transformation of Laguerre–Gaussian laser modes," *Phys. Rev. A, Gen. Phys.*, vol. 45, no. 11, p. 8185, Jun. 1992.

[9] G. R. Guo, W. Hu, and X. Du, "Electromagnetic vortex based radar target imaging," *J. Nat. Univ. Defense Technol.*, vol. 35, no. 6, pp. 71–76, Dec. 2013.

[10] K. Liu, Y. Cheng, Z. Yang, H. Wang, Y. Qin, and X. Li, "Orbital-angular-momentum-based electromagnetic vortex imaging," *IEEE Antennas Wireless Propag. Lett.*, vol. 14, pp. 711–714, 2015.

[11] K. Liu, Y. Cheng, X. Li, Y. Qin, H. Wang, and Y. Jiang, "Generation of orbital angular momentum beams for electromagnetic vortex imaging," *IEEE Antennas Wireless Propag. Lett.*, vol. 15, pp. 1873–1876, 2016.

[12] T. Yang, S. Li, O. Xu, W. Li, and Y. Wang, "Three dimensional SAR imaging based on vortex electromagnetic waves," *Remote Sens. Lett.*, vol. 9, no. 4, pp. 343–352, Apr. 2018.

[13] J. Wang, K. Liu, Y. Cheng, and H. Wang, "Three-dimensional target imaging based on vortex stripmap SAR," *IEEE Sensors J.*, vol. 19, no. 4, pp. 1338–1345, Feb. 2019.

[14] T. Yuan, H. Wang, Y. Qin, and Y. Cheng, "Electromagnetic vortex imaging using uniform concentric circular arrays," *IEEE Antennas Wireless Propag. Lett.*, vol. 15, pp. 1024–1027, 2016.

[15] X. Bu, Z. Zhang, L. Chen, X. Liang, H. Tang, and X. Wang, "Implementation of vortex electromagnetic waves high-resolution synthetic aperture radar imaging," *IEEE Antennas Wireless Propag. Lett.*, vol. 17, no. 5, pp. 764–768, May 2018.

[16] J. Wang, K. Liu, Y. Cheng, and H. Wang, "Vortex SAR imaging method based on OAM beams design," *IEEE Sensors J.*, vol. 19, no. 24, pp. 11873–11879, Dec. 2019.

[17] X. Bu, Z. Zhang, X. Liang, L. Chen, H. Tang, Z. Zeng, and J. Wang, "A novel scheme for MIMO-SAR systems using rotational orbital angular momentum," *Sensors*, vol. 18, no. 10, p. 3511, 2018.

[18] X.-X. Bu, Z. Zhang, L.-Y. Chen, K.-H. Zhu, S. Zhou, J.-P. Luo, R. Cheng, and X.-D. Liang, "Synthetic aperture radar interferometry based on vortex electromagnetic waves," *IEEE Access*, vol. 7, pp. 82693–82700, 2019.

[19] K. Liu, Y. Cheng, X. Li, and Y. Jiang, "Passive OAM-based radar imaging with single-in-multiple-out mode," *IEEE Microw. Wireless Compon. Lett.*, vol. 28, no. 9, pp. 840–842, Sep. 2018.
[20] H. Liu, K. Liu, Y. Cheng, and H. Wang, "Microwave vortex imaging based on dual coupled OAM beams," *IEEE Sensors J.*, vol. 20, no. 2, pp. 806–815, Jan. 2020.
[21] K. Liu, Y. Gao, S. Alkaraki, Y. Cheng, X. Li, and B. Fan, "OAM-generating method based on concentric-ring array using planar antenna," in *Proc. IEEE-APS Topical Conf. Antennas Propag. Wireless Commun. (APWC)*, Sep. 2017, pp. 123–126.
[22] K. Liu, Y. Jiang, Y. Cheng, and X. Li, "Electromagnetic vortex imaging based on distributed OAM radiation sources," in *Proc. Int. Conf. Microw. Millim. Wave Technol. (ICMMT)*, May 2018, pp. 1–3.
[23] T. Yuan, Y. Cheng, H. Wang, and Y. Qin, "Mode characteristics of vortical radio wave generated by circular phased array: Theoretical and experimental results," *IEEE Trans. Antennas Propag.*, vol. 65, no. 2, pp. 688–695, Feb. 2017.
[24] D. Malioutov, M. Cetin, and A. S. Willsky, "A sparse signal reconstruction perspective for source localization with sensor arrays," *IEEE Trans. Signal Process.*, vol. 53, no. 8, pp. 3010–3022, Aug. 2005.
[25] S. Boyd and L. Vandenberghe, *Convex Optimization*. Cambridge, U.K.: Cambridge Univ. Press, 2004.

TAOLI YANG (Member, IEEE) was born in Leshan, China, in 1987. She received the Ph.D. degree in signal processing from the National Key Lab of Radar Signal Processing, Xidian University, China, in 2014. From January 2015 to February 2016, she was a Postdoctoral Research Fellow with the School of Electrical and Electronic Engineering, Nanyang Technological University, Singapore. She is currently an Associated Professor with the School of Resources and Environment, University of Electronic Science and Technology of China. Her current research interests include SAR/ISAR imaging, interferometric SAR, and ground moving target indication.

WEI HUANG was born in Anhui, China, in 1997. He received the bachelor's degree from the Anhui University of Technology (AHUT), China, in 2019. He is currently pursuing the master's degree in electronics and communication engineering with the School of Resources and Environment, University of Electronic Science and Technology of China (UESTC). His current research interests include multi-channel SAR imaging processing and moving target detection.

XINGYU LU was born in Sichuan, China, in 1995. She received the bachelor's degree from the Faculty Geography Resource Sciences, Sichuan Normal University (SICNU), China, in 2018. She is currently pursuing the master's degree with the School of Resources and Environment, University of Electronic Science and Technology of China. Her current research interests include science and technology of surveying and mapping, and InSAR data processing and application.